

Influence of surface defects on the biaxial strength of a silicon nitride ceramic – Increase of strength by crack healing

Walter Harrer^{a,*}, Robert Danzer^a, R. Morrell^b

^a Montanuniversität Leoben, Institut für Struktur- und Funktionskeramik (ISFK), Peter-Tunner Straße 5, A-8700 Leoben, Austria

^b National Physical Laboratory, Teddington, Middlesex, TW11 0LW, United Kingdom

Received 26 April 2011; received in revised form 4 July 2011; accepted 15 July 2011

Available online 30 August 2011

Abstract

Failure of brittle materials starts in general from defects which exist in the volume or on the surface of the specimens. Surface flaws, which are more dangerous than volume flaws, can be introduced by machining. They decrease the strength of specimens and components.

For this investigation silicon nitride specimens were produced using different machining conditions. About half of them were strength tested by use of the biaxial ball-on-three balls (B3B) test. It has been shown that better (more gentle) machining increases the strength but may also cause an increased scatter of strength data.

The remaining specimens were heat treated (annealed) at 1000 °C in air and afterwards also strength tested using the B3B test. Compared to the non heat treated specimens a significant increase in strength could be proven, which was – depending on the machining conditions – between almost 300 MPa and more than 500 MPa. The scatter of strength data was largely decreased.

The improvement was caused by the formation of a thin (0.5–2 µm) glassy layer which filled surface cracks and surface related pores during annealing.

© 2011 Elsevier Ltd. All rights reserved.

Keywords: Strength; Fracture; Si₃N₄; Defects; B3B-test

1. Introduction

The strength of ceramic specimens depends on flaws which exist inside the material or on the surface of the specimen, and which behave similarly to cracks.¹ Unexpected fracture of ceramic components is caused in many cases by surface cracks, which come into existence by lack of attention to machining processes. Therefore a study of the effect of machining conditions (surface quality) on strength and of methods to heal existing machining originated surface cracks is very relevant.

The influence of machining conditions on strength has been investigated some years before by several authors [e.g. 1–4]. During machining of the specimens (and components) grooves (scratches) on the surface are generated by abrasive particles. Commonly these scratches are larger than the material grain size. During machining high temperatures and stresses are generated

in the groove and around the groove local plastic deformations may occur. When the particle moves away from the groove the external load is relaxed and temperatures drop rapidly, often accelerated by the presence of a coolant. Depending on the grinding conditions internal tensile stresses (caused by the preceding plastic deformation) appear and these may be compressive or tensile. If tensile, these stresses can cause the development of parallel, orthogonal and lateral cracks which may decrease the strength of the specimens. Parallel cracks are longer and deeper than orthogonal cracks and therefore typically more severe. Fig. 1 shows a sketch of a surface containing different crack types generated through machining.^{1,3}

Cracks in ceramics can grow if large enough tensile stress components exists perpendicular to the crack boundary. Stress components parallel to the crack plane are more or less harmless. Therefore stresses in the machining direction (which are perpendicular to the less deep orthogonal cracks) are less dangerous than stresses perpendicular to the machining direction (which are perpendicular to the deeper parallel cracks).

Some work (especially on Si₃N₄, SiC and SiC/Si₃N₄ composites) has been reported to find a heat treatment to improve

* Corresponding author. Tel.: +43 38424024110, fax: +43 3842 402 4102.
E-mail address: Walter.Harrer@mu-leoben.at (W. Harrer).

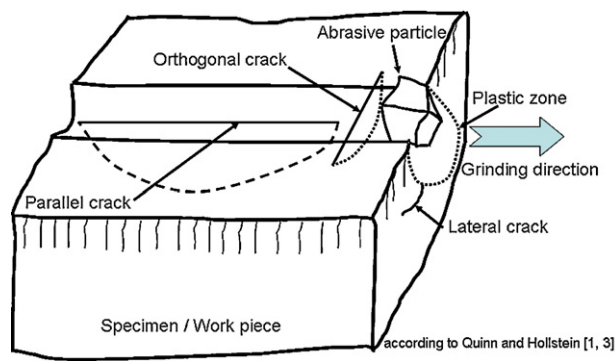


Fig. 1. During machining of brittle materials parallel, orthogonal and lateral cracks can become into existence. Also lateral cracks, which are oriented parallel to the surface and start at the plastic zone, may be part of the crack system.⁸ Parallel cracks have a greater length and depth than orthogonal cracks. Therefore they are also more severe than the other types of cracks.⁷

the strength of machined specimens [e.g. 5–9]. In silicone nitride ceramics a suitable annealing of specimens in air causes to the formation of thin surface oxide layers (e.g. SiO₂ and Y₂Si₂O₇) which may heal surface cracks and may increase the strength of the annealed specimens.^{5–10}

In general strength testing of ceramics is made in (3-point or 4-point) bending¹¹ of rectangular bars, which are machined out of larger pieces of material. In the tested bars a uniaxial stress state exists. In order to minimise the influence of machining on the test outcome (attempting to measure the “material’s strength”) standards demand that grinding of specimens has to be made in the longitudinal direction of the specimens. The deep longitudinal machining cracks are then in the “harmless” direction and only the small orthogonal cracks tend to influence the results of the strength measurement.

But in service ceramic components are often loaded in a biaxial stress state (e.g. during a thermal shock), where, for cracks of any direction, large stress components perpendicular to the crack plane exist and, therefore, cracks of any direction are dangerous. In this paper a study of the influence of surface conditions (after grinding, lapping or polishing and after annealing to heal surface cracks) on the biaxial strength of a commercial silicon nitride material is made.

2. Experimental procedure

2.1. Strength testing

More than ten years ago some reviews on methods for biaxial strength testing were made.^{12,13} For several reasons (load transfer, friction, data evaluation based on simple beam theory, ...) these methods are not very precise. Recently a new biaxial strength test (the ball-on-three balls or B3B test), which is very simple and much more precise, has been developed. Therefore the B3B-test is used for this investigation. In the B3B-test a disc shaped specimen is positioned on three balls and centrally loaded by a fourth ball. It is important to note that the maximum tensile stress appears in a relatively small area (in our case with a radius a few hundred µm) in the centre of the

Table 1
Some mechanical properties of the investigated silicon nitride material.

Young’s modulus <i>E</i> (GPa)	Vickers-hardness HV5 (GPa)	Fracture toughness <i>K_{IC}</i> (MPa m ^{0.5}), SEVNB-method	Density <i>ρ</i> (kg/m ³)
297 ± 2	15.5 ± 0.3	5.0 ± 0.2	3203 ± 1

disc on the opposite side of the loading ball, where the biaxial stress state exists. Theoretical background, evaluation, experimental procedure and possible measurement inaccuracies are described in Refs. [14–16]. For comparison some additional tests were made by conventional 4-point bending testing following EN 843-1.¹¹

In total 260 B3B-test specimens and 45 bending test specimens were tested.

2.2. Investigated material, sample preparation and annealing

The investigated material is a commercial gas pressure sintered silicon nitride with Alumina and Ytria additives produced by FCT Ingenieurkeramik, Germany (trade name FSNI). In Table 1 some mechanical properties (measured at ISFK) of the material are given. The Young’s modulus was measured in three point-bending after EN 843-2, the density was measured by use of the Archimedes principle (EN 623-2).

The specimens for the B3B tests were cut out of large discs (diameter 250 mm, thickness 5 mm) and had a diameter of ~20 mm and a thickness of approximately ~2 mm (delivered by FCT Ingenieurkeramik). The tensile loaded surfaces of the specimens of samples A–G were machined in different ways at ISFK, see Table 2, and those of (H) were lapped by the supplier. All samples were initially ground using a D46 wheel (500 µm of material was removed), and for a D15 ground condition a further 25 µm of material was removed with a grit size of 15 µm.

For bending tests specimens (≥45 mm × 4 mm × 3 mm) were cut from the same type of discs at ISFK. The surface of the bending specimens was machined according EN 843-1¹¹ using a grinding wheel (resin bonded) with a diamond grit size of 15 µm.

To get a first impression on the surface quality conventional roughness measurements of the surfaces were performed in two (perpendicular) directions with a roughness measurement device Surtronic 3 from Taylor & Hobson (measuring tip radius 5 µm), see Table 2. Note that these data probably underestimate the true roughness by a small amount because of the larger than recommended tip radius employed (EN623-4 recommends 2 µm).

144 of the B3B-specimens were strength tested in the as-machined conditions and 116 B3B-specimens were annealed to perform some surface crack healing before testing. These specimens were heated up to 1000 °C in air in an electric furnace with a ramp rate of 5 °C/min. The exposure time was 10 h. To distinguish the as-machined from annealed samples the sample and the specimen identifiers were given prefixes (*n*) and (*a*), respectively.

Table 2

Sample numbers, machining steps for surface finishing and average surface roughness R_a before and after annealing in air at 1000 °C.

Sample	Machining parameters	Average surface roughness R_a /ten-point height R_z (μm) not annealed (n)	Average surface roughness R_a /ten-point height R_z (μm) annealed (a)
A (B3B)	Ground, grit size 46 μm (D46)	0.23/1.51	0.19/1.29
B (B3B)	Ground, grit size 15 μm (D15), used wheel	0.11/0.99	0.10/0.80
C (B3B)	Ground, grit size 15 μm (D15) dressed wheel	0.06/0.46	0.08/0.59
D (B3B)	D46, D15 and then polished to 9 μm	0.03/0.21	0.05/0.39
E (B3B)	D46, D15 and then polished to 6 μm	0.04/0.17	0.04/0.29
F (B3B)	D46, D15 and then polished to 3 μm	0.01/0.10	0.05/0.35
G (B3B)	D46, D15 and then polished to 1 μm	0.01/0.11	0.05/0.33
H (B3B)	Lapped, B ₄ C, F 600 (FEPA standard) grain size 3–18 μm	0.19/2.74	0.14/0.96
4PB (4-point-bending)	Ground, grit size 15 μm (D15)	0.09/0.88	0.14/0.90

3. Results and microscopic analysis

3.1. Comparison of specimen surfaces before and after annealing

Fig. 2 shows parts of the surfaces from specimens of samples B (ground, D15, used wheel) before and after annealing (SEM image, large magnification). During annealing and under the given conditions the formation of yttrium-containing crystals (white spots) appeared on the surface. However, as will be shown later, these “first” crystals have no influence on the strength of the specimens.

To show the effect of crack-healing Vickers indentations (HV5) were made into five specimens with polished surfaces (sample G, 1 μm, compression side), see Fig. 3a. After annealing (Fig. 3b) some crack healing can be recognised.

3.2. Strength test results

Table 3 shows a summary of the results of the strength measurements. The data were evaluated according to the Weibull theory using the maximum likelihood method (e.g. following EN 843-5,¹⁷). Given is the number of tested specimens per sample, the characteristic strength (the stress, where 63% of the specimen fails) and the Weibull modulus, which is a measure for the width of the distribution of the size of the fracture origins (the wider the distribution, the smaller the modulus).

Fig. 4 shows the characteristic strength for the performed biaxial strength tests (samples A–H). For comparison the characteristic strength of the bending tests is also shown. It is well known that there exists a size effect on strength.^{18,19} Therefore the bending test data shown in Fig. 4 were converted to the size and stress state of the B3B specimens using the principle of independent action. A short outline of this procedure can be found in the Appendix.

It is obvious that machining has a strong impact on strength and that annealing generally increases the strength.

In Fig. 5 the Weibull moduli of the tested samples are shown. The modulus of the as-machined (not annealed) specimens depends strongly on the machining conditions (Fig. 5a), but the modulus of the annealed samples (Fig. 5b) is more consistent

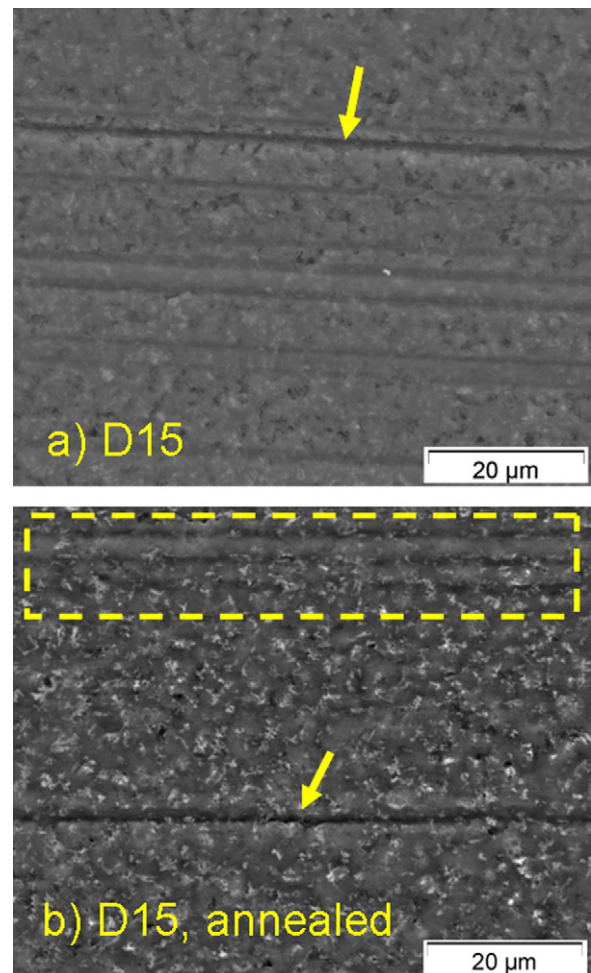


Fig. 2. SEM-micrographs from the surface of a specimen of sample B, which was ground with 15 μm (D15) (a) before and (b) after annealing. One deep scratch (arrow) and several smaller scratches were found on the surface before annealing. After annealing a scratch on the surface, which was too deep to be healed, can still be recognized. The rectangle marks several other scratches which were healed. On the surface white spots can be recognized. Through an EDX-analysis it was found that these spots contain a high concentration of yttrium.⁶

Table 3

Strength test results of the investigated samples. The values in the squared brackets refer to the 90% confidence intervals.

Sample (annealed/not annealed)	Number of tested spec.	Char. strength σ_0 (MPa)	Weibull modulus m (–)
n-A	15	728 [692–767]	9.9 [6.3–12.8]
a-A	15	1245 [1180–1315]	9.3 [6.0–12.1]
n-B	30	858 [830–886]	10.3 [7.7–12.5]
a-B	15	1368 [1324–1414]	15.3 [9.8–20.0]
n-C	15	1011 [953–1075]	8.4 [5.3–10.9]
a-C	15	1455 [1398–1516]	12.4 [8.0–16.2]
n-D	15	1068 [979–1169]	5.7 [3.6–7.4]
a-D	14	1351 [1268–1441]	8.3 [5.2–10.8]
n-E	15	1056 [993–1126]	8.0 [5.1–10.4]
a-E	15	1425 [1356–1501]	10.0 [6.4–13.0]
n-F	15	990 [878–1120]	4.2 [2.7–5.4]
a-F	15	1279 [1197–1370]	7.5 [4.8–9.8]
n-G	25	1048 [979–1123]	5.5 [3.9–6.8]
a-G	13	1465 [1414–1520]	15.3 [9.4–20.2]
n-H	14	865 [769–977]	4.4 [2.8–5.8]
a-H	14	1208 [1143–1279]	9.4 [5.9–12.3]
n-4PB	30	839 [815–864]	11.5 [8.6–14.0]
a-4PB	15	1012 [981–1045]	15.9 [10.2–20.7]

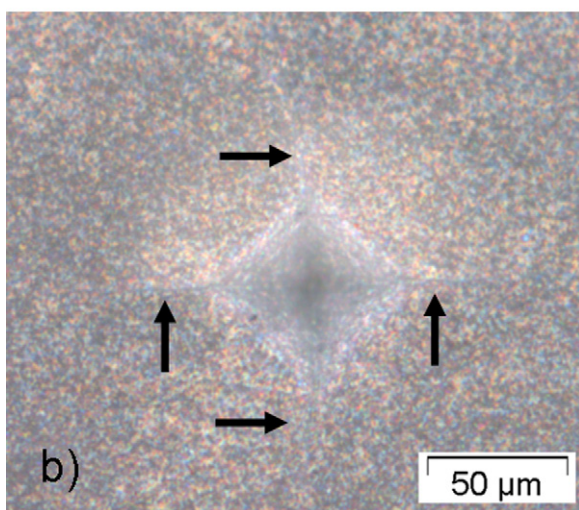
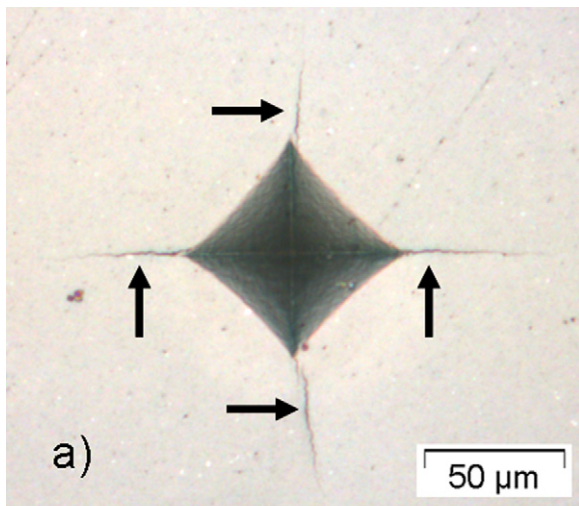


Fig. 3. Vickers indentation (HV5) on the surface of a polished specimen before (a) and same indentation after (b) annealing. The arrows indicate the cracks starting from the indentations.

(the 90% confidence intervals of the data overlap; with only one of ten values excepted).

3.3. Fractography

To identify possible fracture origins and for a better understanding of the test results an in-depth fractographic analysis was performed on selected fractured specimens from all samples. Before testing the areas where fracture is expected to originate (i.e. where the maximum tensile stress appears) were investigated to document possible machining damage for all specimens. An example for a not annealed specimen with different surface flaws is shown in Fig. 6.

After testing the Griffith defect^{21,22} size

$$a_c = \frac{1}{\pi} \cdot \left(\frac{K_c}{Y\sigma_f} \right)^2 \quad (1)$$

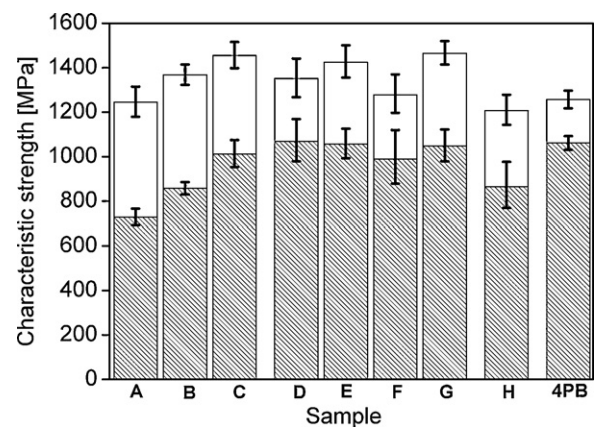


Fig. 4. Strength test results of samples prepared with different surface finishing. The filled bars (hatched) show the results for the non-annealed samples, the open bars represent the annealed samples. The scatter bars show the 90% confidence intervals on the obtained values. For a better comparison the bending test data were converted to the size and stress state of the B3B-data (and therefore are higher than the values given in Table 3).

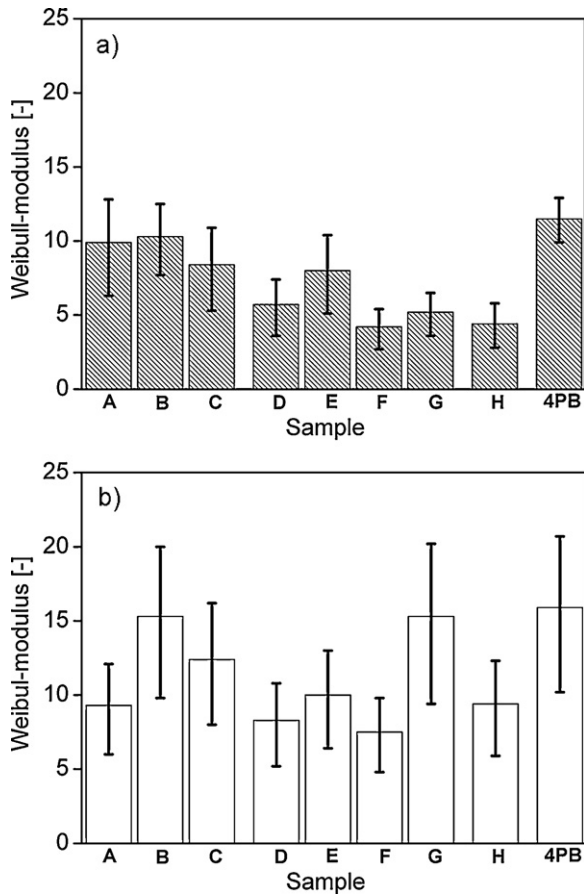


Fig. 5. Weibull-modulus of the tested samples (left side not annealed samples, right side annealed samples). The scatter bars show the 90% confidence intervals.

of all specimens were calculated in order to realise the size of critical flaws, which helps to analyse the microscopic findings. For the fracture toughness K_{IC} , the value of Table 1 was used. Since fracture from machining flaws was expected to occur, the geometric factor of small elongated surface cracks (edge through-cracks, $Y = 1.12$) was used. σ_f is the strength of the specimen. Typical values of the Griffith crack size (i.e. depth) for the as-machined (not heat treated) specimens range from 5 μm to 15 μm and for the heat treated specimens from 2 μm to 4 μm .

For the not annealed samples typical fracture origins are shown in Figs. 7–9.

For the annealed samples typical fracture origins are shown in Figs. 10 and 11. In any analysed specimen a glassy surface layer with a thickness of 0.5–2 μm was found. At the fracture surfaces some secondary damage could be found in some cases but typical features like mirrors or hackle lines were missing in most cases.

4. Discussion

It should be noted that the statistical nature of failure of ceramics makes a statistical analysis of data necessary. The sample is always different to the parent distribution, but confidence intervals can be determined. To give an example, if a 90% confidence interval for the characteristic strength value (or for the Weibull modulus) is given, then the probability is 90% that the characteristic strength (or the Weibull modulus) of the parent distribution is within the limits of this interval. This also implies that in one of ten samples, it is expected to be outside of this interval. The width of this interval becomes wider the smaller the sample size (i.e. number of tested specimens) is. To properly

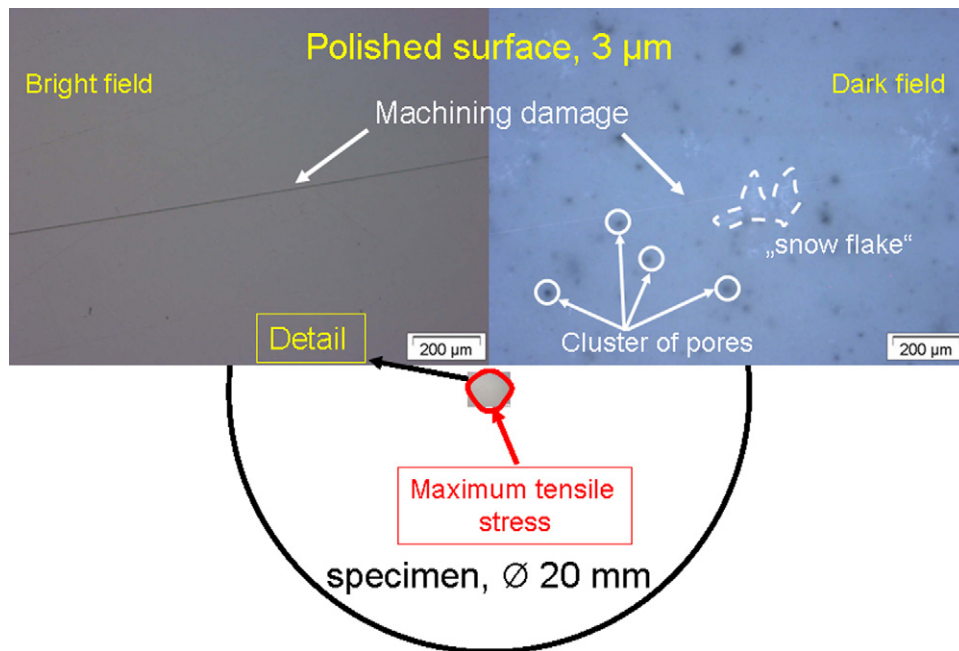


Fig. 6. Machining damage and “natural” defects on the tensile surface of a polished specimen of sample a–F (the pictures show the centre of the disc, i.e. the area where the maximum tensile stress occurs). Defects like clusters of micro pores or snow flakes (which only can be recognized in a dark field illumination²⁰) can also limit the strength if they are large enough and situated in the centre of the specimen.

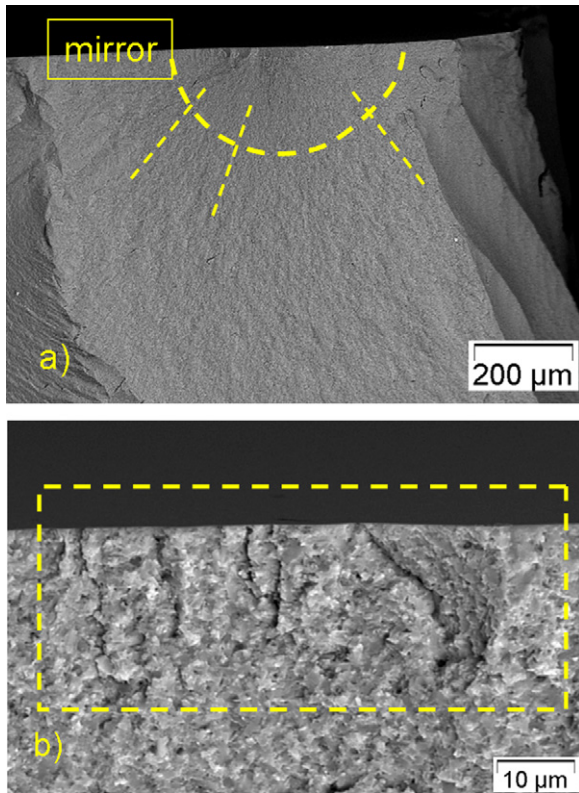


Fig. 7. Fracture surface of a fragment of specimen n-G6. This specimen's surface was polished down to 1 μm. (a) Mirror and hackle lines indicate that fracture started at or near the surface. (b) A crack system similar to a coarse “zipper crack”, which is typical for transversely-ground or scratched specimens,²³ was found in this area.

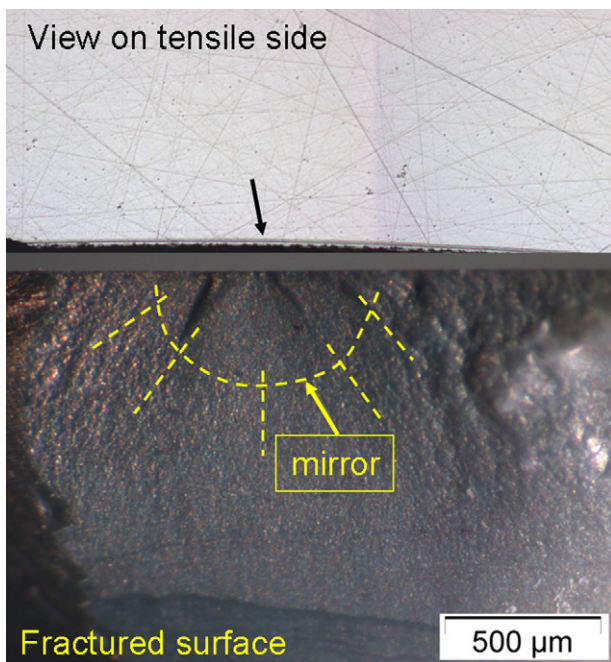


Fig. 8. View on the tensile side and on the fracture surface (same scale, the picture was made up of one light microscope and one stereo microscope micrograph) of a fragment of specimen n-D9. Failure starts at a scratch (arrow) which was introduced through machining of the tensile side.

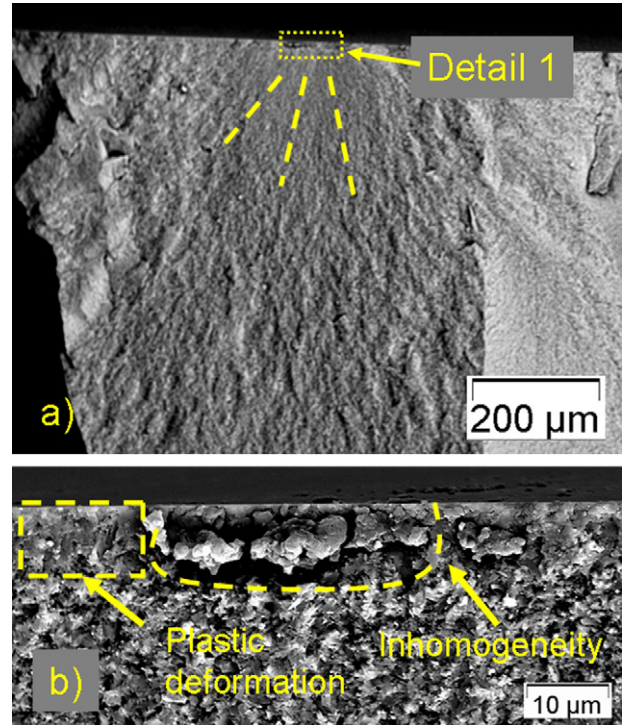


Fig. 9. Fracture surface of one fragment of specimen n-F7: (a) overview of the mirror region and (b) fracture origin of specimen in a high magnification in the SEM. The origin is a surface located elongated Si_3N_4 -agglomerate which is surrounded by a pore. Such agglomerates are a remnant of spray-dried granulates.

determine a strength (Weibull) distribution, a very large sample would be necessary.

4.1. Strength of as-machined (not annealed) samples

The biaxial strength of the as-machined tested samples is strongly dependent on the machining conditions (see Table 3 and Fig. 4). The strength is relatively low if grinding is made with a coarse grained wheel (sample n-A, ground with D46, $\sigma_0 = 728$ MPa) or is done with an imperfectly dressed wheel (sample n-B, ground with D15, used wheel, $\sigma_0 = 858$ MPa). In the case of grinding with a D15 dressed wheel (n-C) or when the surface is polished after grinding (n-D to n-G) the surface damage is reduced and the strength is increased. In these cases σ_0 ranges from 990 MPa to 1068 MPa, or in other words, within the

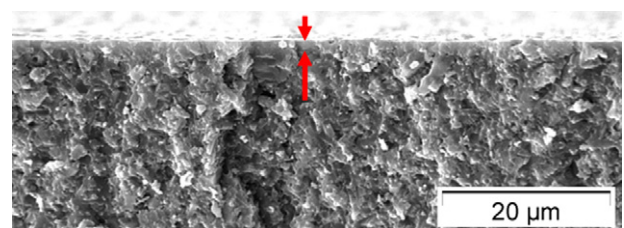


Fig. 10. SEM-micrograph of the fracture surface of one fragment of specimen a-C23. A glassy layer (indicated by arrows) with a thickness of 0.5–2 μm has been formed during annealing.

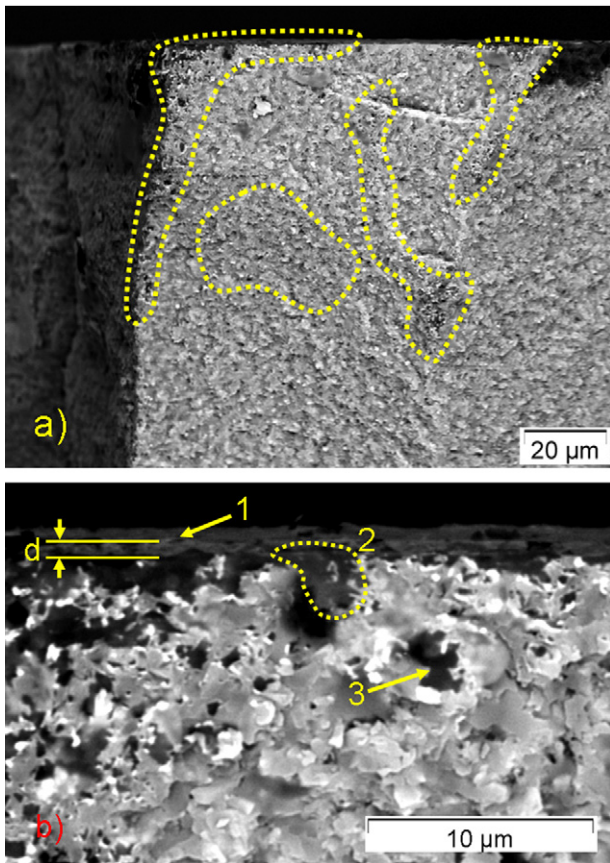


Fig. 11. Fracture surface of one fragment of specimen a-A20: (a) cluster of micro pores on the tensile surface and in the volume. (b) At a higher magnification a glassy layer (1) with a thickness (d) in the range of $0.5\text{--}2\text{ }\mu\text{m}$ can be recognized on the surface. At a surface located pore the glassy layer extends into the pore, partly filling and sealing it (2). Of course pores within the volume (3) cannot be healed.

90% confidence limits the characteristic strength of the samples is very similar in these tests.

In the case of the lapped specimens (sample n-H) the surface quality is strongly dependent on the handling of the process and of the action of a few large lapping grains, which may cause large scratches and a loss of strength. In fact the characteristic strength is as low as 865 MPa.

The bending specimens have a characteristic strength of 839 MPa. In order to assess these data it must be recognised that the stressed surface area in the bending specimens is much larger than the B3B specimens. Since there is a size effect on strength of ceramics a fair comparison of B3B test results and bending test results needs an extrapolation of the characteristic bending strength to the strength of a the B3B specimens (for details see the Appendix), which yields about 1060 MPa. This strength is higher than most of the values of the biaxial tested samples.

The strength test results are also supported by fractographic analysis. In the samples where the grinding conditions were rough (with D46 and D15) a large amount of machining induced defects can be found on the ground surfaces (n-A to n-C; see Fig. 2a). These defects cause a strong decrease of strength (compared to the polished specimens), which is even more severe due

to the biaxial stress state. The high density of surface cracks of similar depth causes a relatively high Weibull modulus; its value is around 10 for these samples. The modulus of the polished (and of the lapped samples n-D to n-G) is much lower (around 5). The microscopic analysis shows some large scratches (see Figs. 6 and 8), which will cause early fracture and a low strength, if they are in the area of very high tensile stresses (in the centre of the B3B disc), but which are not relevant for strength, if they are away from this area. Note that at the stress level corresponding to the characteristic strength 63% of the specimens fail but 37% survive (these specimens fail at higher stresses). Therefore the few scratches, which cause a low strength in a fraction of the specimens, have only a small influence on the characteristic strength, but they cause a very low modulus.

Because in the B3B-test only a small volume fraction is loaded under high tensile stress it is unlikely to contain significant volume located flaws.²⁴ In most cases “natural” flaws, which act as fracture origins are surface located or near-surface located.

In the case of the as-machined samples there exists a good accordance between surface roughness and strength, which means that a higher surface roughness leads to a lower strength.³

4.2. Strength of annealed samples

During annealing a thin glassy layer and some yttrium-containing crystals have been generated on the surface of the annealed samples (e.g. see Fig. 2b, Fig. 10 or Fig. 11). While the crystals are too small to have significant influence on mechanical properties, the glassy layer fills and blocks the micro pores and the machining induced flaws and heals these defects at least partially (if they are not too deep). As a result a significant increase of the characteristic biaxial strength of the B3B-samples (and also of the strength of the uniaxial bending tests) can be observed. The annealed B3B samples showed – compared to the as-machined samples – an increase in the characteristic strength by almost 300 MPa (samples n-D, n-F) to more than 500 MPa (samples n-A, n-B). The Weibull modulus is similar (around 10) for all annealed samples (at the 90% confidence level).

During the strength experiments the annealed specimens broke into many fragments and shards (commonly the number of fragments increases with the stored elastic energy), therefore it was difficult to identify typical fracture origins. The fracture origins which could be identified, were surface or near surface located flaws like clusters of micro-pores (as shown in Fig. 11) or inhomogeneities (similar to the Si_3N_4 -agglomerate in Fig. 9). Origins which might be machining flaws could not clearly be identified as fracture origins.

Even in the case of the annealed specimens the samples with the highest surface roughness (a-A, a-H) had the lowest strength,³ reflecting the importance of the original surface topography.

5. Conclusions

The quality of the surface has a very strong influence on the strength of the specimens. In the case of the investigated

silicon nitride specimens with surfaces machined using several different but commonly employed grinding or polishing procedures, the differences in the characteristic strength exceeded 300 MPa. Therefore the manner of machining of components may be decisive for their reliability.

To determine the bending strength of materials the standards generally require grinding parallel to the specimen's longitudinal direction, where the influence of machining on strength is expected to be minimal, but such a benign situation only rarely occurs in real applications. Therefore, in general, the bending test result overestimates the strength of components. A more appropriate testing procedure for design data acquisition purposes would be an uniaxial bending test with specimens machined perpendicular to the longitudinal direction or a biaxial strength test. Therefore we conclude that the B3B test is a good test to measure design relevant strength data.

In the case of the biaxial strength tests made on ground and then polished specimens, the characteristic strength was significantly increased, but the scatter of strength data was also increased. In some parts of the surface the deep grinding cracks could not completely be polished out. This shows that the original grinding has still some influence on strength, which will be more severe, if large specimens having a large stressed surface area are evaluated. It follows that the complete removal of heavy grinding damage is needed if strength is to be enhanced by subsequent lapping or polishing.

The heat treatment procedure applied to the investigated silicon nitride has been shown to be a very effective way to increase the strength of our specimens. An increase in the characteristic strength of up to 500 MPa could be observed for several specimen batches. Therefore it is concluded that the reliability of components can, in principle, also significantly be increased by such a thermal treatment provided that the oxide layer remains intact, undamaged, and is not removed by corrosive environments.

In the samples where rough machining caused deep machining damage and a low characteristic strength (samples A and H), the characteristic strength after the aging procedure is still a little lower than for the other samples. This shows that the healing could not be completely remove deep subsurface damage in these cases.

Appendix A. Appendix: Extrapolation of 4-point bending strength data to B3B strength data

The 4-point bending test has a uniaxial and the B3B test has a biaxial stress field, which is used for strength determination. The biaxial stress field is more testing of machining damage than the uniaxial stress field. Therefore an equivalent stress has to be defined to take the stronger action of the biaxial stress field into account.

Several proposals for the definition of the equivalent stress exist, but the differences in outcome are small and the scatter of experimental data is large. Therefore no consensus on the proper definition of the equivalent stress yet exists. In the following we use the principle of independent action criterion (PIA), in which

the action of each principal stress component (σ_I , σ_{II} and σ_{III}) is added:

$$\sigma_{eq,PIA} = (\sigma_I^m + \sigma_{II}^m + \sigma_{III}^m)^{1/m} \quad (A1)$$

m is the Weibull-modulus of the material. For the biaxial stress state in the middle of the B3B specimen it holds: $\sigma_I = \sigma_{II}$ and $\sigma_{III} = 0$ and the equivalent stress is: $\sigma_{eq,PIA} = 2^{1/m} \cdot \sigma_I$. For a uniaxial stress state, as it exists in a bending bar, the equivalent stress is: $\sigma_{eq,PIA} = \sigma_I$. The higher equivalent stress in the biaxial stress state compared to the uniaxial state thus accounts for its more damaging action.

It is also well known that the strength of ceramic specimens depends on their size (size effect on strength). The characteristic strength of large specimens is lower than that of small specimens, since the probability of finding a large flaw in a large specimen is higher than in a small specimen. This fact is described in the Weibull theory.^{25,26} In our actual case with small test pieces we analyse the action of surface flaws. Therefore the size effect of strength depends on the (effective) surface of the specimens. For the characteristic strength (σ_1 and σ_2 respectively) of specimens having the (effective) surface S_1 and S_2 respectively it holds:

$$\sigma_2 = \sigma_1 \cdot \left(\frac{S_1}{S_2} \right)^{1/m} \quad (A2)$$

The effective surface S_{eff} is defined by:

$$S_{eff} = \int_{\sigma > 0} \frac{\sigma_{eq}(\vec{r})^m}{\sigma_{ref}^m} dS \quad (A3)$$

σ_{ref} is a reference stress, which is chosen to be equal to the maximum principal stress in the specimen. The effective surface corresponds to the surface of the specimen where the highest tensile stresses occur and depends on the Weibull modulus m .

The extrapolation of the bending test results to the conditions of B3B testing has been made on the basis of the above equations. For more details see Ref. [27].

References

1. Quinn GD, Ives LK, Jahanmir S. On the nature of machining cracks in ground ceramics: a case study on silicon nitride. NIST Special Publication; 2003. p. 996.
2. Rice RW, Mecholsky Jr JJ, Becher PF. The effect of grinding direction on flaw character and strength of single crystal and polycrystalline ceramics. *J Mater Sci* 1981;16:853–62.
3. Hollstein T, Pfeiffer W, Rombach M, Thielicke B. Analysis of machining damage in engineering ceramics by fracture mechanics. In: Varner J, Fréchet V, Quinn G, editors. *Fractography of glasses and ceramics III, ceramic transactions, vol. 64*. Ohio: Westerville; 1996. p. 145–69.
4. Pfeiffer W, Hollstein D. Influence of grinding parameters on strength-dominating near – surface characteristics of silicon nitride ceramics. *J Eur Ceram Soc* 1997;17:487–94.
5. Clarke DR, Lange FF. Strengthening of a sintered silicon nitride by a post-fabrication annealing. *J Am Ceram Soc* 1982;65:C51–2.
6. Zhang YH, Edwards L, Plumbbridge WJ. Crack healing in a silicon nitride ceramic. *J Am Ceram Soc* 1998;81:1861–8.
7. Ando K, Takahashi K, Nakayama S, Saito S. Crack healing behaviour of Si₃N₄/SiC ceramics under cyclic stress and resultant fatigue strength at the healing temperature. *J Am Ceram Soc* 2002;85:2268–72.
8. Houjou K, Ando K, Liu SP, Sato S. Crack-healing and oxidation behaviour of silicon nitride ceramics. *J Eur Ceram Soc* 2004;24:2329–48.

9. Nakatani M, Ando K, Houjou K. Oxidation behaviour of $\text{Si}_3\text{N}_4/\text{Y}_2\text{O}_3$ system ceramics and effect of crack-healing treatment on oxidation. *J Eur Ceram Soc* 2008;**28**:1251–7.
10. Lube T. Improvement of the strength of silicon nitride by aging. *Fract Mech Ceram* 2002;**13**:151–8.
11. EN 843-1: *Advanced technical ceramics, monolithic ceramics-mechanical properties at room temperature, part 1: determination of flexural strength*; 1995.
12. Morrell R, McCormick NJ, Bevan J, Lodeiro M, Margetson J. Biaxial disc flexure – modulus and strength testing. *Brit Ceram Trans* 1999;**98**:234–40.
13. Godfrey DJ, John S. Disc flexure tests for the evaluation of ceramic strength. In: *Ceramic materials and components for engines*. Lübeck-Travemünde; 1986. p. 657–65.
14. Börger A, Supancic P, Danzer R. The ball on three balls test for strength testing of brittle discs: stress distribution in the disc. *J Eur Ceram Soc* 2002;**22**:1425–36.
15. Börger A, Supancic P, Danzer R. The ball on three balls test for strength testing of brittle discs: part II: analysis of possible errors in the strength determination. *J Eur Ceram Soc* 2004;**24**:2917–28.
16. Harrer W, Danzer R, Supancic P, Lube T. Influence of the sample size on the results of B3B-tests. *Key Eng Mater* 2009;**409**:176–84.
17. EN 843-5: *Advanced technical ceramics, monolithic ceramics-mechanical properties at room temperature, part 5: statistical evaluation*; 1997.
18. Danzer R. A general strength distribution function for brittle materials. *J Eur Ceram Soc* 1992;**10**:461–72.
19. Danzer R. Some notes on the correlation between fracture and defect statistics – are Weibull-statistics valid for very small specimens. *J Eur Ceram Soc* 2006;**26**:3043–9.
20. Herrmann M, Schulz I, Bales A, Sempf K, Hoehn S. Snow flake structures in silicon nitride ceramics-reasons for large scale optical inhomogeneities. *J Eur Ceram Soc* 2008;**28**:1049–56.
21. Irwin GR. Analysis of stresses and strains near the end of a crack traversing plate. *J Appl Phys* 1957;**24**:361–4.
22. Munz D, Fett T. *Ceramics: mechanical properties, failure behaviour materials selection*. Berlin: Springer-Verlag; 1999.
23. Quinn GD. *Fractography of ceramics and glasses*. Washington: NIST Special Publication; 2007. p. 960–16.
24. Freudenthal A. A statistical approach to brittle fracture. *Fracture* 1968:591–619.
25. Weibull W. *A statistical theory of strength of materials*. Stockholm: Royal Swedish Institute for Engineering Research; 1939. p. 1–45.
26. Weibull W. A statistical distribution function of wide applicability. *J Appl Mech* 1951;**18**:293–7.
27. Danzer R, Lube T, Supancic P, Damani R. Fracture of ceramics. *Adv Eng Mater* 2008;**10**:275–98.